Lasers in Manufacturing Conference 2013

Experimental investigation of laser transmission welding of thermoplastics with part-adapted temperature fields

M. Devrient*[a], M. Kern[b], P. Jaeschke[b], U. Stute[b], H. Haferkamp[b], M. Schmidt[a,c,d]

[a]*blz Bayerisches Laserzentrum GmbH, Erlangen*
[b]*LZH Laser Zentrum Hannover e.V., Hannover*
[c]*LPT Chair of Photonic Technologies of the Friedrich-Alexander Universitaet Erlangen-Nuernberg, Erlangen*
[d]*SAOT Erlangen Graduate School in Advanced Optical Technologies, Erlangen*

Abstract

Laser transmission welding is known for high flexibility, extraordinary potential for process automation and outstanding weld seam properties. Problems may occur due to the poor gap-bridging capability of contour welding. Gaps of a few tens of microns can lead to processing issues such as welding failures, poor achievable process speed or low weld seam strengths. To overcome this, laser transmission welding with part-adapted temperature fields was developed, and is experimentally investigated here. Results concerning the process behavior, dependent on several oscillation types of the laser beam, as well as achieved tensile shear strengths and the monitored gap-bridging capability are presented.

Keywords: laser transmission welding; thermoplastics; laser beam oscillation; tensile shear strengths; gap-bridging capability

1. Motivation / State of the Art

Laser transmission welding requires the laser energy to pass through the upper joining partner of an overlap or T joint, and be absorbed by the lower joining partner, near the joining plane in between the parts (cp. Fig. 1 left). Thereby, heat is generated, and the parts are welded together at the joining plane. Proper process parameters and sufficient clamping pressure are both necessary in order to perform high-quality

---

* Corresponding author. Tel.: +49 (0) 9131 97790-28; Fax: +49 (0) 9131 97790-11.
E-mail address: m.devrient@blz.org

welds. When relatively large parts must be joined, today's contour welding process technology is limited due to small unbridgeable gaps, on the order of less than 50 μm dependant on various parameters relevant to the process [1]. These gaps may exist even with adequate clamping. When local gaps remain, the heat generated in the lower part is not sufficiently conducted to the upper one, which can result in welding failures, poor achievable process speed, and low weld seam strength. Laser transmission welding of thermoplastics with part adapted temperature fields introduced by [2, 3] seems to be a promising approach to achieve a welding process similar to contour welding but with an improved gap-bridging capability. Therefore further investigations are performed.
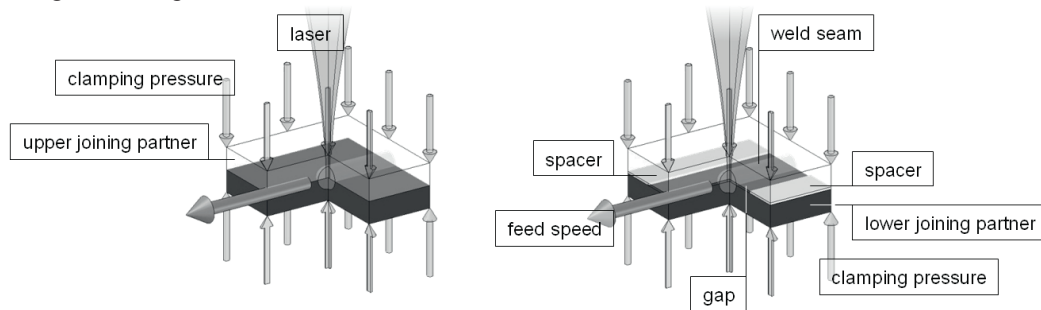

Fig. 1. The procedural principle of laser transmission welding (left) and the experimental setup chosen to determine the gap-bridging capability (right)

As demonstrated in prior research [1, 4, 5, 6], an elongation of the melt pool by the use of a line-like intensity distribution [1, 4], or a double focus configuration [5, 6], yields better gap-bridging capability. Forming a longer melt pool at the same feed speed, there is more time for heating, melting, interaction within the collective melt pool, cooling and the solidification of the molten material.

Here, instead of using static optical components, a scanning system implements highly dynamic laser beam oscillation [3]. This beam guidance distributes the laser energy spatially and temporally in a well-defined manor, resulting in precisely-tailored intensity distributions. Using a robotically-operated scanning system, part adapted temperature fields become achievable for use with bigger parts and with a three dimensional weld seam contour [3]. The melt pool geometry of this process, as well as the achievable braking forces and tensile shear strengths need to be further investigated and compared to conventional contour welding. It must be determined, if the gap-bridging capability of this approach can be improved, relative to contour welding. Furthermore the possibility and accuracy of temperature measurements by the use of an on-axis mounted high speed pyrometer for the purpose of process control and quality assurance have to be determined.

2. Experimental

For this research, an experimental investigation of laser transmission welding of thermoplastics with part-adapted temperature fields is performed and temperature measurement experiments are carried out. The weld seam width, achievable breaking forces, tensile shear strengths, and gap-bridging capabilities of laser transmission welding with part-adapted temperature fields are determined, with regard to their dependency on different beam oscillation types and varying process parameters. These characteristics are determined for PMMA- (polymethylmethacrylate), PE- (polyethylene) and PA 6-samples (polyamide) arranged in overlap configurations with varying gap thicknesses defined by spacers with varying thicknesses (cp. Fig. 1 right).

The temperature measurement experiments are performed for PE-samples. Here, relative temperatures are determined, with regard to their dependency on different scan speeds and a mimicked defect geometry.

2.1. Experimental setup for the welding experiments

The welding experiments are carried out by the use of a 350 W diode laser provided by Trumpf Laser. The beam source emits at a central wave length of 980 nm. The fibre used for guiding the laser radiation to the scanning system has a core diameter of 150 µm and a numerical aperture of 0.22. Furthermore the experimental setup is consisting of three orthogonal arranged linear stages, with an assured repeatability of ± 5 µm and a maximum travelling speed of 250.0 mm s^{-1} for each stage. The scanning system, a Raylase superscan 20 with an assured repeatability of ± 10 µrad, is connected to a f-theta objective, a Sill S4LFT2163/094. The clamping device can be used with a simple glass plate or a clamping latch with slits allowing the laser beam to reach the clamped work pieces directly and vice versa the emitted temperature radiation to reach the off-axis mounted thermo camera, a Thermosensorik CMT 384 SM as well in a direct way. Fig.2. is showing an image of the setup.
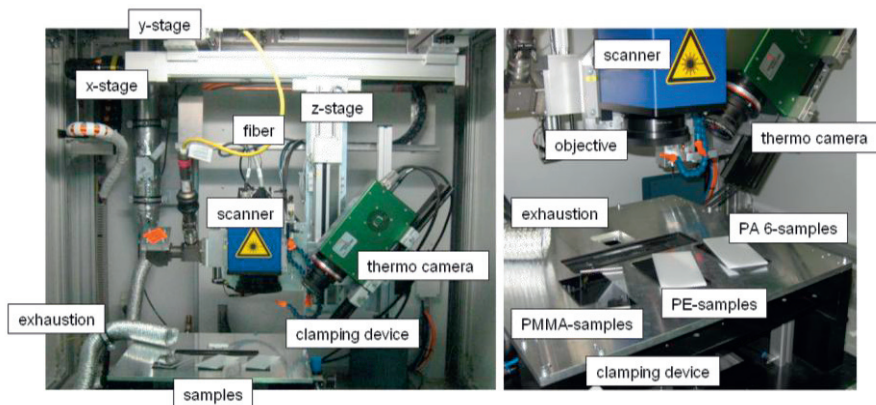

Fig. 2. Image of the experimental setup chosen for the welding experiments

As mentioned the samples used for the welding experiments are made out of PMMA, PE and PA 6. The samples acting as upper joining partner are unfilled, the samples taken as lower joining partner are filled with carbon black. The filling degree used is unknown but expected to be > 1 % per weight. The dimensions of the samples (cp. Fig. 2 left) are 120.0 mm times 60.0 mm times 3.0 mm. The sample thickness of 3.0 mm is defined within an extrusion process, the other dimensions are defined by sawing. The overlap of the samples is chosen to be 40.0 mm times 120.0 mm. The spacers used are made out of stainless steel. Their thickness, defines the gap thickness in between the two joining partners and varies from 5 µm to 150 µm. Their width, measured orthogonal to the direction of movement of the feed speed $v_{s,cont.}$ is 12.5 mm. Their length, is chosen to be more than 120.0 mm. To assure a constant gap thickness along the linear welding contour, the spacers are arranged symmetrically to the plane defined by the direction of $v_{s,cont.}$ and the laser beam axis of the not oscillating laser beam.

2.2. Welding experiments

To determine the weld seam width, achievable breaking forces, tensile shear strengths and gap-bridging capabilities of laser transmission welding with part-adapted temperature fields, with regard to their dependency on different beam oscillation types and varying process parameters the samples are welded under the no gap condition (cp. Fig. 1 left), as well as with the mentioned spacers in between the upper and the lower joining partner (cp. Fig. 1 right). By using spacers with varying thickness, varying gap thicknesses are realized. The process parameters considered beside the gap thickness and the different oscillation types are

laser power P_L, focal position relative to the joining plane Δz, feed speed $v_{s,cont.}$ and scan speed $v_{s,scan}$, which drives the laser beam oscillation. The experiments are performed with a constant clamping pressure of 0.15 N mm^{-2} related to the pressurized surface. Within the experiments, the gaps' thickness is successively increased from the no-gap condition until 150 µm. The resulting weld seam width, achievable breaking forces and tensile shear strengths are quantified, dependent on their respective gap thickness. The gap thickness for which the tensile shear strength reaches 80% of the value reached under the no gap condition is declared to exhibit a gap-bridging capability [4]. To compare laser transmission welding with part-adapted temperature fields to conventional contour welding, this procedure is carried out using different types of beam oscillation, as well as no laser beam oscillation. Welding with no laser beam oscillation represents conventional contour welding. For each parameter combination three samples are welded. Concerning the laser beam oscillation three oscillation types: circular, elliptic and lemniscate like oscillation are considered. Fig. 3 is showing the shape of the intensity distributions resulting from the different oscillation types and the intensity distributions of the not oscillating beam as well.
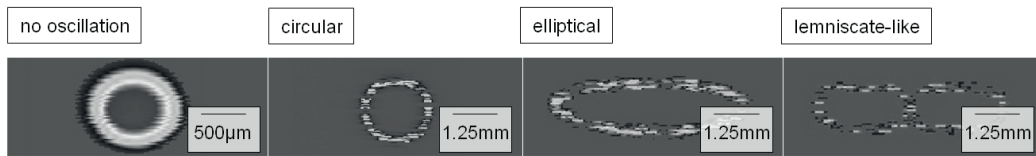

Fig. 3. Shapes of the intensity distributions resulting for the different oscillation types monitored by measurements with a hollow needle instrument within the focal plane; $v_{s,cont.} = 0.0$ mm s^{-1}; $v_{s,scan} = 1{,}000$ mm s^{-1}; $\Delta z = 0.0$ mm and $P_L = 24.4$ W

For the monitoring a hollow needle instrument, a Primes Focus Monitor is used [7]. Within the measuring field of the hollow needle instrument, which is chosen to be equal to the focal plane, 128^2 data sets of the spatial coordinates x and y and the spatial monitored average intensities are collected. For the measurement in one measuring field the scanning system is performing a continuous laser beam oscillation, while the laser is emitting continuously at a constant laser power. The measuring field dimensions are chosen to be maximum 4.0 mm times 6.0 mm. Therefore the spatial resolution for the performed measurements in x-direction is at least 32 µm and in y-direction 47 µm.

Fig. 4 is showing the shape of the intensity distributions resulting from the oscillation type elliptical, when $v_{s,scan}$ is varied.
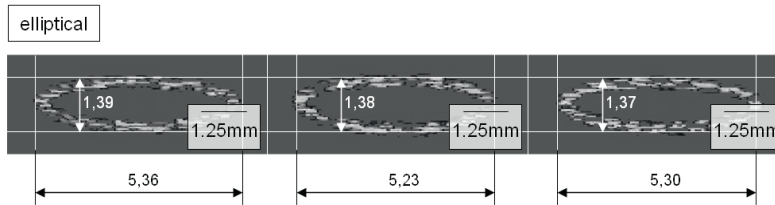

Fig. 4. Dimensions and shapes of the intensity distributions resulting from the elliptical oscillation type monitored by measurements with a hollow needle instrument within the focal plane; $v_{s,cont.} = 0.0$ mm s-1; $v_{s,scan} = 800$ mm s-1 (left), 1,000 mm s-1 (middle) and 1,200 mm s-1 (right); $\Delta z = 0.0$ mm and $P_L = 24.4$ W

The dimensions of the intensity distributions are compared for different oscillation types and for varying scan speeds. It is obvious that for the considered $v_{s,scan}$-values only a slight change of the dimensions b, orientated in direction of the later weld seam width and l, orientated collinear to the direction of $v_{s,cont.}$ can be stated.

In a first series of welding experiments the parameters P_L, Δz, $v_{s,cont.}$ and $v_{s,scan}$ are varied for each material combination and oscillation type using a single factor design. For this series no spacers are used. For

each varied parameter, a local maximum in the tensile shear strength is detected, under no-gap condition, also showing the best weld seam appearance. Fig. 5 is exemplarily showing tensile shear strengths concerning the material PMMA and the oscillation type circular with varying parameters of the P_L, $\nu_{s,cont.}$ and $\nu_{s,scan}$.
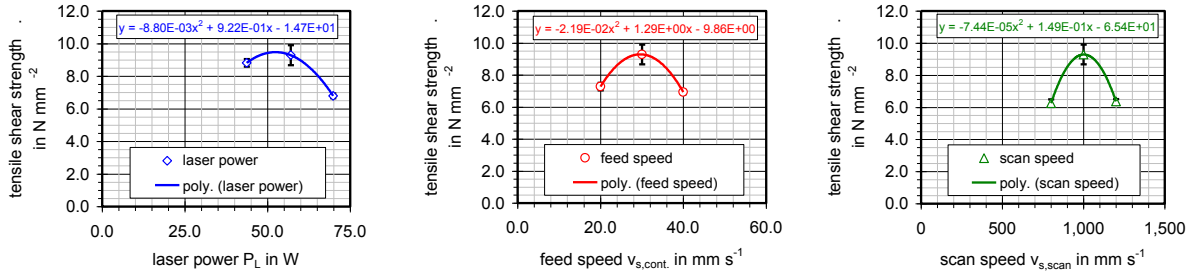

Fig. 5. Exemplarily diagrams showing the tensile shear strength determined for PMMA-samples dependant on P_L (left), $\nu_{s,cont.}$ (middle) and $\nu_{s,scan}$ (right) for the oscillation type circular; all results shown in this figure are determined under no gap condition using a single factor design; left: Δz = 20.0 mm; $\nu_{s,cont.}$ = 30.0 mm s^{-1}; $\nu_{s,scan}$ = 1,000 mm s^{-1}; middle: P_L = 57.0 W; Δz = 20.0 mm; $\nu_{s,scan}$ = 1,000 mm s^{-1}; right: P_L = 57.0 W; Δz = 20.0 mm; $\nu_{s,cont.}$ = 30.0 mm s^{-1}

Along side the detection of parameter sets leading to a local optimum also some comparison of laser transmission welding with part-adapted temperature fields and conventional contour welding can be made. For all materials and oscillation types the feed speed $\nu_{s,cont.}$ leading to a local optimum concerning the weld seam appearance and tensile shear strength in case of laser transmission welding with part-adapted temperature fields e.g. is higher or at least equal to $\nu_{s,cont.}$ leading to a local optimum concerning the weld seam appearance and tensile shear strength for conventional contour welding rather the welding with no laser beam oscillation. The determined laser power P_L is always higher for a welding process with laser beam oscillation than without. By laser beam oscillation a longer and wider melt pool is formed [3], therefore more power is needed. Comparing the determined focal position relative to the joining plane Δz, no significant difference for the welding experiments with and without laser beam oscillation can be stated. Nevertheless for Δz = 0.0 mm the effect of laser beam oscillation onto the weld seam cross section and the formed temperature field becomes most obvious e.g. when observing the welding process with the of-axis mounted thermo camera [3].
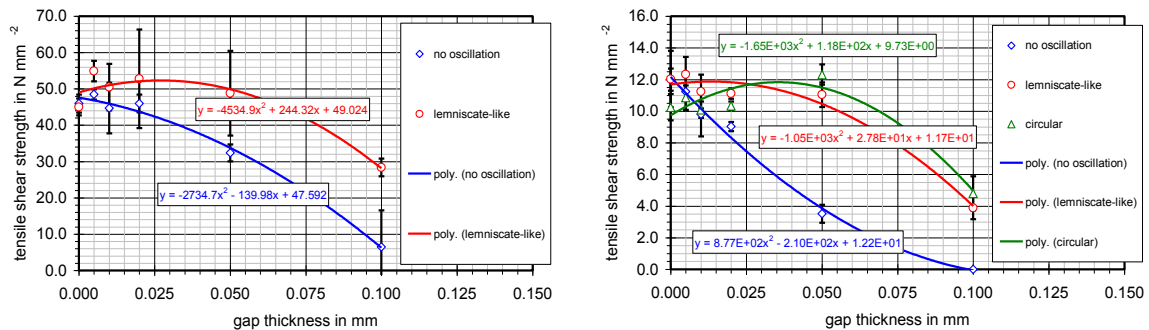

Fig. 6. Exemplarily diagrams showing the tensile shear strength determined for PA 6- (left) and PMMA-samples (right) dependant on the gap thickness; left: no oscillation: P_L = 30.3 W; Δz = 20.0 mm; $\nu_{s,cont.}$ = 20.0 mm s^{-1}; left: lemniscate-like oscillation: P_L = 63.5 W; Δz = 20.0 mm; $\nu_{s,cont.}$ = 20.0 mm s^{-1}; $\nu_{s,scan}$ = 1,200 mm s^{-1}; right: no oscillation: P_L = 26.9 W; Δz = 20.0 mm; $\nu_{s,cont.}$ = 30.0 mm s^{-1}; right: lemniscate-like oscillation: P_L = 56.9 W; Δz = 20.0 mm; $\nu_{s,cont.}$ = 40.0 mm s^{-1}; $\nu_{s,scan}$ = 1,200 mm s^{-1}; right: circular oscillation: P_L = 53.7 W; Δz = 20.0 mm; $\nu_{s,cont.}$ = 30.0 mm s^{-1}; $\nu_{s,scan}$ = 1,000 mm s^{-1}

After detecting parameter sets leading to local ideal weld seam appearance and tensile shear strength for each material combination and oscillation type under the no gap condition, these parameters are used for a second series of welding experiments with continuously increasing gap thickness. Fig. 6 is showing exemplarily the tensile shear strengths diagrams obtained for two (PA 6 and PMMA) of the three considered materials and two (circular and lemniscate-like) of the three considered oscillation types. The result is compared to the tensile shear strength obtained for no laser beam oscillation. As it can be seen in Fig. 6, for both materials and oscillation types the gap-bridging capability can be increased by the laser beam oscillation. Interesting might be, that the maximum tensile shear strength is obtained for a several micrometer gap thickness and not exclusively under the no gap condition. A result, reminding to the fact that laser transmission welding is dependant on the three state variables: time, temperature and pressure [8]. Comparable results are documented but not discussed by [4] for contour welding experiments with a point-shaped and a line-like intensity distribution and the material polypropylene (PP). Tab. 1 summarizes the obtained gap-bridging capabilities for the considered materials and oscillation types taken into account and compares the values to the obtained gap-bridging capabilities for no laser beam oscillation rather contour welding.

Table 1. Gap-bridging capabilities obtained for PMMA-, PE- and PA 6-samples for no laser beam oscillation, circular, elliptical and lemniscate-like laser beam oscillation

Material	Oscillation type	Gap thickness respective to the max. tensile shear strength determined	Calculated gap-bridging capability (linear interpolation)	Improvement of the calculated gap-bridging capability relative to no laser beam oscillation
PMMA	no oscillation	0 μm	11 μm	-
PMMA	circular	50 μm	81 μm	736 %
PMMA	lemniscate-like	5 μm	63 μm	573 %
PE	no oscillation	0 μm	8 μm	-
PE	elliptical	5 μm	26 μm	318 %
PE	lemniscate-like	0 μm	15 μm	177%
PA 6	no oscillation	5 μm	38 μm	-
PA 6	lemniscate-like	5 μm	75 μm	197 %

Regarding *Fig. 5* and *Tab. 1* it becomes obvious, that for laser transmission welding with laser beam oscillation, higher tensile shear strength and a better gap-bridging can be achieved compared to the process with no laser beam oscillation. Regarding the industrial application of laser transmission welding with part-adapted temperature fields, this seems to be a very promising result.

2.3. Experimental setup for the temperature measurement experiments

Furthermore, welding experiments with a circular temperature field are carried out, using PE-samples and a pyrometric system, used for a simultaneous on-axis thermal radiation detection. The samples acting as upper, laser transmitting joining partner are unfilled. The lower, laser absorbing joining partner is filled with carbon black. The filling degree used here is unknown. The dimensions of the injection molded samples are 100.0 mm times 25.0 mm times 1.0 mm. The overlap of the samples here is chosen to be 50.0 mm times 25.0 mm. The clamping pressure is 0.1 N mm^{-2}. Here a 300 W diode laser provided by Laserline is used. This beam source is emitting at a central wave length of 940 nm. The fibre used for guiding the laser radiation to

the scanning system has a core diameter of 400 µm and a numerical aperture of 0.22. Furthermore the experimental setup is consisting of a linear stage. The scanning system, a Raylase turboscan 30 with an assured repeatability of ± 10 µrad is combined with an f-theta objective, the Sill S4LFT0202/094. Furthermore a clamping device and an on-axis mounted high speed pyrometer, the Sensotherm Metis HI18 are used. *Fig. 7* (left) is showing an overview of the described experimental setup used for the laser transmission welding experiments with simultaneous thermal radiation detection.
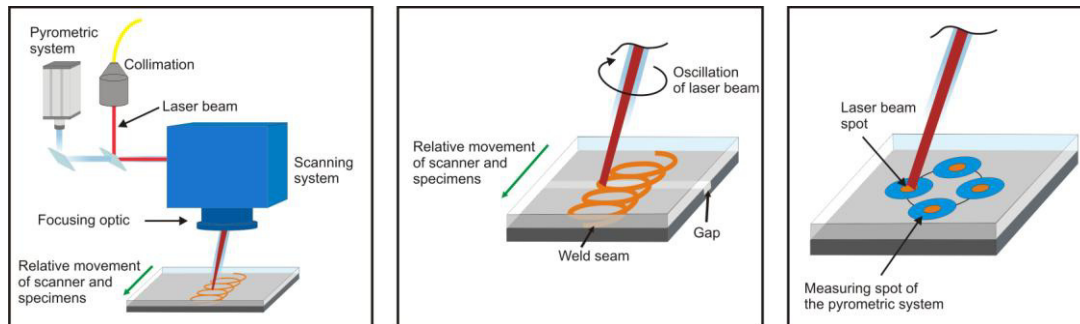

Fig. 7. Experimental setup of laser transmission welding with simultaneous thermal radiation detection (left), a description of the arrangement of the gap in the surface of the absorbing plastic (middle) and the experimental setup to ensure the laser spot to be centered in the measuring spot of the pyrometric system (right)

Carrying out the temperature measurement experiments, the scanning system implements a circular laser beam oscillation with a diameter d_c of 10.0 mm. At the same time the clamped joining partners are moved relatively to the scanning system by the linear stage with a constant feed speed $v_{s,cont.}$ of 10.0 mm s^{-1}. During the welding process, the laser heated and partial molten plastics, emit thermal radiation in each direction. A part of this radiation reaches the pyrometric system travelling back the optical path of the laser beam (cp. *Fig. 7* left). Both, the laser beam and the thermal radiation, have to pass the scanning system, the focusing optic and the upper joining partner, but in reverse order. As shown in *Fig. 7* left the pyrometric system is coupled to the optical path of the laser beam by a semi-transparent mirror. This mirror reflects the laser beam with a wavelength λ of 940 nm under 90°, relative to its optical path, while enabling the thermal radiation to transmit to the pyrometric system. Before reaching the pyrometric detector, the thermal radiation is deflected by an adjustable mirror. Therewith the optical path of the thermal radiation can be aligned to the optical path of the laser beam to detect the thermal radiation emitted at the very position of the present laser beam position on the joining partners. The pyrometric system detects infrared radiation in a spectral range from $\lambda = 1.65$ µm to $\lambda = 2.10$ µm and temperatures between $T = 120$°C and $T = 520$°C. All experiments are carried out with a sample rate of $f = 7$ kHz of the pyrometric system.

The pyrometric systems output value is a temperature. This value is dependent upon the emission coefficient of the emitting plastics, the area of the detected thermal emission and the intensity of the thermal radiation. However, the thermal radiation is attenuated by the partial absorption of the upper, laser transmitting plastic and the focusing optic on its path to the pyrometric detector. Taking into account the attenuation of the thermal radiation, the measured temperature does not represent the real temperature of the joining plane, but is referred to as relative temperature T_{rel} in this investigation.

Similar to the welding examples also for the temperature measurement experiments a non-color-corrected f-theta objective is used. This objective is configured for the wavelength of the laser beam and not for the spectral rage of the pyrometric system. For this reason optical aberrations of the thermal radiation and the laser beam need to be taken into account. Since the index of refraction of the focusing optic varies with the

wavelength of the radiation, two kinds of chromatic aberrations occur: Axial and lateral aberration. As a result of the axial aberration, the focal positions of radiations with dissimilar wavelengths do not coincide. The consequence for radiation with dissimilar wavelengths, which are deflected off the optical axis of an optic, is to strike a plane at slightly different positions, due to the lateral aberration.

Within the temperature measurement experiments the laser beam is focused right onto the joining plane in between the two joining partners ($\Delta z = 0.0$ mm). As a consequence of the axial aberration, the measuring spot of the pyrometric system does not reach its minimal possible size, but a diameter of $d_P = 4.8$ mm. When applying a circular laser beam oscillation with a diameter of $d_c = 10.0$ mm the lateral aberration of the laser beam and the detected thermal radiation is less than $a_L = 0.1$ mm, for all wavelength, detected by the pyrometric system. Therewith, the lateral aberration between the wavelength of the laser beam and the detected thermal radiation, is small, compared to the laser beam spot diameter of $d_L = 1.3$ mm and the diameter of the measuring spot of the pyrometric system. Therefore the lateral aberration can be disregarded for the temperature measurement experiments, because it is too small to prevent the laser beam spot and the measuring spot of the pyrometric system to coincide.

2.4. Temperature measurement experiments

Using the described setup an experiment is applied to ensure the laser beam spot to be centered in the measuring spot of the pyrometric system (cp. *Fig. 7* right). Therefore, four equidistant positions on the circumference of the circle performed by the laser beam oscillation are chosen. On each of these four positions an energy output is generated by the laser for the same period of time. At the same time, the thermal radiation of each of the four positions is recorded by the pyrometric system. The arithmetic average of the relative temperature of each of the four positions is $T_{rel} = 232.3$°C. The standard deviation is $\sigma_T = 1.6$°C. Hence it can be stated, that the laser beam and the optical path of the pyrometric system are well aligned for the laser transmission welding investigations.

Going ahead within this research, varying scan speeds $v_{s,scan}$ of the circular oscillation of the laser beam, as well as mimicked defects in the welding contour and their effects on the temperature signal are investigated. Therefore, gaps are created in the surface of the lower, absorbing plastic (cp. *Fig. 7* middle). The gaps have a width w and thickness d of 1.0 mm and are perpendicular to the relative movement of the scanning system and the plastics to be welded. When investigating the scan speed $v_{s,scan}$ of 50 mm s^{-1}, a laser power of $P_L = 20.0$ W is applied. For the scan speed $v_{s,scan}$ of 100 mm s^{-1} a laser power P_L of 30.0 W is set.

For laser transmission welding with a circular beam oscillation and simultaneous thermal radiation detection, a periodic pattern in the relative temperature signal can be observed (cp. *Fig. 8*). Out of the elapsed time between two neighbored local minima of the relative temperature signal and the circumference of one circle performed by the laser beam oscillation, a scan speed $v_{cal.}$ can be calculated. For this scan speed, the arithmetic average is determined for the complete weld seam length of each welding sample. The arithmetic average of the calculated speed corresponds well with the set scan speed $v_{s,scan}$. For a scan speed $v_{s,scan}$ off 50 mm s^{-1} the calculated speed $v_{cal.}$ reaches a value of 51.2 mm s^{-1} and a standard deviation of 4.3 mm s^{-1}. For $v_{s,scan} = 100$ mm s^{-1}, $v_{cal.}$ is determined to be 100.2 mm s^{-1}, showing a standard deviation of 9.7 mm s^{-1}. Hence, it can be concluded, that on-axis thermal radiation detection through a scanning system and a non-color-corrected f-theta objective is feasible for laser transmission welding with laser beam oscillation.

The local minima in the temperature signal (cp. *Fig. 8*) are considered to represent the front of the temperature field, in the direction of the relative movement of the scanning system and the plastics to be joined. Here, due to the combination of feed $v_{s,cont.}$ and scan speed $v_{s,cont.}$, the laser beam gets in contact with sections of the plastics that have not been crossed in a prior turn of the laser beam oscillation driven by $v_{s,scan}$. These sections are therefore not preheated. As result, the temperature signal decreases, in contrast to those

sections of the plastics that have already been passed by the laser beam in prior turns and that are therefore preheated when the laser beam crosses these sections again. Accordingly these preheated sections are showing higher relative temperatures.
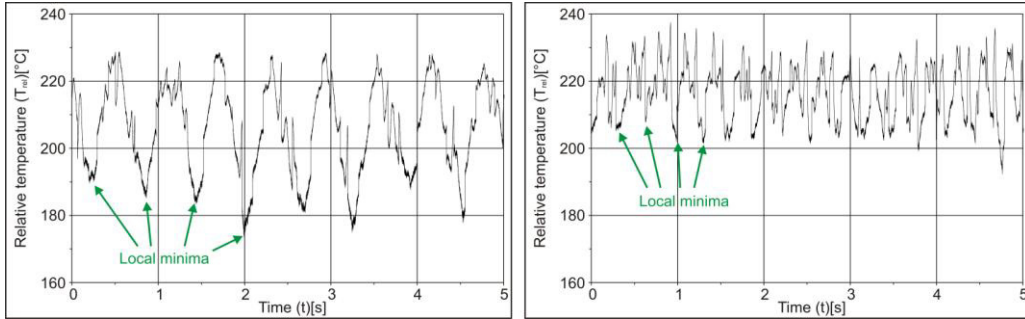

Fig. 8. Relative temperature signal of the thermal radiation detection during laser transmission welding without a gap in the joining plane of the plastics; with a scan speed of $v_{s,scan}$ = 50 mm s^{-1} (left) and a scan speed of $v_{s,scan}$ = 100 mm s^{-1} (right)

Due to the constant feed speed $v_{s,cont.}$ and the set laser power of P_L = 30.0 W, do the samples, welded with a scan speed of $v_{s,scan}$ = 100.0 mm s^{-1}, show an increased average relative temperature of $T_{rel,a}$ = 216.4°C, compared to the samples welded with a scan speed of $v_{s,scan}$ = 50 mm s^{-1} and the reduced laser power of P_L = 20.0 W. For these samples an average relative temperature of $T_{rel,a}$ = 206°C during the laser transmission welding is determined. Defects in the joining plane, mimicked by gaps in the lower plastic are investigated. As for welding samples that do not have a gap in the joining plane, a periodic pattern in the relative temperature signal can be observed for the samples that have a gap (cp. *Fig. 9*).
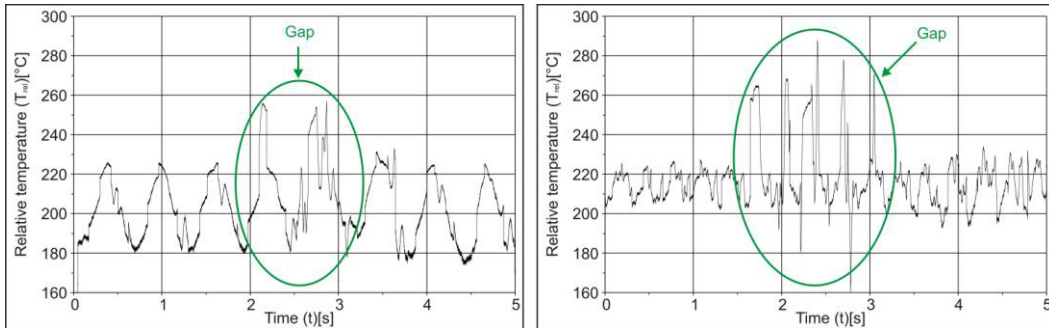

Fig. 9. Relative temperature signal of the thermal radiation observation during laser transmission welding with a gap in the joining plane of the plastics to weld; using a scan speed of $v_{s,scan}$ = 50 mm s^{-1} (left) and a scan speed of $v_{s,scan}$ = 100 mm s^{-1} (right)

This periodic pattern can be observed before and after the gap, but also when the laser beam crosses the gap. Thereby the calculated scan speed $v_{cal.}$ still corresponds with the set scan speed $v_{s,scan}$-values. The amplitude of the relative temperature signal before and after the gap is comparable with those samples, that are processed with the same scan speed but without a gap in the joining plane. But when the laser beam crosses the gap, a general increase of the amplitude of the relative temperature signal $T_{rel,b}$ becomes apparent, for both scan speeds $v_{s,scan}$. The increase of the amplitude of the relative temperature can be explained by the reduction of the thermal conductivity between the laser absorbing and the laser transmitting plastic at the gap [9]. The thermal conductivity of an air filled gap is less than that of PE. Therefore a heat built-up develops at the gap and is detected by the pyrometric system.

3. Summary

An experimental investigation of laser transmission welding of thermoplastics with part-adapted temperature fields is presented. Therefore the shapes and dimensions of the different intensity distributions resulting from the different laser beam oscillation types circular, elliptical and lemniscate-like are investigated by measurements with a hollow needle instrument. It was shown, that the scanning system is able to form intensity distributions with nearly constant dimensions for different scan speed values relevant for the performed welding experiments.

After detecting welding parameter settings leading to a local maximum in the tensile shear strength under the no-gap condition, the gap-bridging capability for different sample materials and oscillation types was determined relative to the welding with no laser beam oscillation. The maximum improvement of the gap-birding capability was achieved for PMMA performing a circular laser beam oscillation.

An on-axis temperature detection through a non-color-corrected f-theta objective for laser transmission welding with part adapted temperature fields is presented as well. Addressing a circular temperature field by an oscillating beam guidance, a periodic temperature signal is detected by the pyrometric system, matching with the set scan speed. Gaps in the surface of the laser absorbing plastic are detected. They implicate a heat built-up in the joining plane, due to the reduced thermal conductivity of the air filled gap in comparison with the plastics. As result, an increase in the measured temperature signal is detected.

Based on these results, further investigations need to be performed in order to reduce the diameter of the measuring spot of the pyrometric system to enable a more precise temperature detection and therewith the implementation of smaller temperature fields. This can be achieved by an increased aperture of the pyrometric system, but is limited to the aperture of the scanning system. Further investigations are focusing to establish a quality control strategy based on the pyrometric signal, in order to prevent decompositions in the weld seam and to constantly reach the melting point temperature of the plastics, even when surface failures of the plastics occur or a bad clamping of the plastics hamper the welding process.

References

[1]   Frick, T.: Untersuchung der Prozessbestimmenden Strahl-Stoff-Wechselwirkung beim Laserstrahlschweißen von Kunststoffen, Dissertation, Universität Erlangen-Nürnberg, 2007.

[2]   Devrient, M.: Laserstrahlschweißen von Thermoplaste mit bauteilangepassten Temperaturfeldern. In: Laser Magazin 29 (2012) 4, Hightech Publications KG, Bad Nenndorf, 2012, p. 28.

[3]   Devrient, M.; Wippo, V.; Frick, T.; Jaeschke, P.; Stute, U.; Haferkamp, H.; Schmidt, M.: Laser transmission welding with part adapted temperature fieldp. In: Proceedings of the 31st International Congress on Applications of Lasers and Electro-Optics (ICALEO 2012), Anaheim, USA (California), 2012, p. 826-834.

[4]   Haensch, D.: Die optischen Eigenschaften von Polymeren und ihre Bedeutung für das Durchstrahlschweißen mit Diodenlasern. Dissertation, Universität Aachen, 2001.

[5]   Jaeschke, P.; Herzog, D.; Haferkamp, H.: Influence of the beam forming and the intensity distribution on the process limits in the process of laser transmission welding. In: Joining Plastics 1, 2009, p. 42-48.

[6]   Fargas, M.: Erweiterung des Prozessverständnisses beim Laserstrahldurchschweißen von Thermoplasten durch Analyse der Schmelzbaddynamik. Dissertation, Universität Hannover, 2012.

[7]   Schwede, H.; Urmoneit, U.: Charakterisierung von fokussierter Laserstrahlung im industriellen Umfeld zur Qualitätssicherung. In: Tagungsband des Fachseminars Laser in der Elektronikproduktion & Feinwerktechnik 2002 (LEF 2002), Meisenbach Verlag, Bamberg, 2002, p. 85-92.

[8]   Michel, P.: Schweißverfahren in der Kunststoffverarbeitung - Grundlagen und Aspekte zur Serienfertigung. Habilitation, Universität Paderborn, 1999.

[9]   Wippo, V.; Devrient, M.; Kern, M.; Jaeschke, P.; Frick, T.; Stute, U.; Schmidt, M.; Haferkamp, H.: Evaluation of a pyrometric-based temperature measuring process for the laser transmission welding. In: Proceedings of the 7th International Congress on Laser assisted near net shape ingeniering (LANE 2013), Fuerth, Germany, published by Physics Procedia 39, 2012, p. 128-136.